Standardization of Second-Order Instruments

Yongdong Wang and Bruce R. Kowalski*

Laboratory for Chemometrics, Center for Process Analytical Chemistry and Department of Chemistry, BG-10, University of Washington, Seattle, Washington 98195

A method is presented to standardize two-dimensional responses (e.g., GC/MS, LC/UV) measured on multiple instruments or on a single instrument under different operational conditions. This second-order standardization method proceeds by calculating two banded diagonal transformation matrices, using the responses of a common standard sample, to simultaneously correct for the response channel shift and intensity variations in both dimensions or orders. Different from first-order standardization, these two transformation matrices must be estimated from a set of simultaneous nonlinear equations via the Gauss-Newton method. The effects of noise and transformation matrix bandwidth on the standardization performance are studied through computer simulation. When tested with experimental LC/UV data, the proposed standardization method can reduce the variation between two runs from 0.15-0.20 to 0.025-0.03 AU. From both the computer simulation and experimental data study, it is found that the design of the standard sample is critical for the parameter estimation and response standardization.

INTRODUCTION

In previous publications,[1-3] various standardization methods have been reviewed and presented for multivariate calibration, to either correct for response variations or adjust the calibration model so that it can be applied to another instrument producing different responses. These standardization methods were developed for so-called first-order instruments (e.g., spectrometers) that produce a vector of data per sample. They were not intended for second-order instruments[4,5] (e.g., GC/MS) that are capable of generating a matrix of data for each sample analyzed. Though more powerful than first-order calibration in terms of analytical capacity, second-order calibration is more prone to response variations, which can now occur in both orders simultaneously. For example, the second-order data collected from liquid chromatography with ultraviolet spectroscopic detection (LC/UV) can have a shift in retention time, due to temperature and pressure fluctuations and column aging, as well as a wavelength shift in the UV spectrometer and a spectroscopic intensity variation, due to the misalignment of the monochromator and light source intensity changes. To make things worse, when such instrumental variations occur in second-order data, it is difficult to decide whether the variations come from one order or the other or both. This makes it difficult to apply first-order standardization separately in each order to standardize a second-order instrument. It is therefore necessary to assume that one order is stable while the other order is being standardized. For example, in an experimental employing thin-layer chromatography with a diode array detector, Burns et al. attempted to solve the retention time irreproducibility problem through explicit peak shape modeling under the assumption that the spectrometer was stable from run to run.[6]

In this paper, a general second-order standardization method is developed and tested to standardize both orders simultaneously and thereby achieve second-order calibration transfer. Though second-order calibration transfer was the primary motivation for this work, second-order standardization can also be used for other purposes. One example is the interlaboratory comparison and validation of second-order instruments, which has been an extremely difficult task.[7]

THEORY

Method Development. In first-order piecewise direct standardization (PDS),[1] the responses of a small set of transfer samples measured on two different instruments are related to one another through a banded diagonal matrix $\mathbf{F}$ (for continuous responses),

$$\bar{\mathbf{R}}_1 = \bar{\mathbf{R}}_2\mathbf{F} \tag{1}$$

where $\bar{\mathbf{R}}_1$ and $\bar{\mathbf{R}}_2$ are the matrices containing instrument responses in the rows. This banded diagonal matrix $\mathbf{F}$ is arranged in such a way that the response at every specific channel on the first instrument can be represented as a linear combination of the responses in a small window near this specific channel on the second instrument. The linear combination can accomplish corrections of both response channel shifts and intensity changes.

When the second-order response of a sample, $\mathbf{N}_1$ (dimensioned $m \times n$), measured on one instrument is compared to the response of the same sample, $\mathbf{N}_2$ (dimensioned the same as $\mathbf{N}_1$), on another instrument, it is expected that the differences will occur in both orders. To correct for such complicated differences, two transformation matrices similar to $\mathbf{F}$ are needed. This leads to the following nonlinear form in which the responses of the common sample from both instruments are related to one another via a left and right transformation matrix, $\mathbf{A}$ and $\mathbf{B}$,

$$\mathbf{N}_1 = \mathbf{A}\mathbf{N}_2\mathbf{B} \tag{2}$$

The left transformation $\mathbf{A}$ will correct for shift and intensity differences between the rows of $\mathbf{N}_1$ and $\mathbf{N}_2$ (e.g., standardizing the LC order) with the following banded diagonal form

* To whom correspondence should be addressed.

(1) Wang, Y.; Veltkamp, D. J.; Kowalski, B. R. *Anal. Chem.* **1991**, *63*, 2750.
(2) Wang, Y.; Lysaght, M. J.; Kowalski, B. R. *Anal. Chem.* **1992**, *64*, 562.
(3) Wang, Y.; Kowalski, B. R. *Appl. Spectrosc.* **1992**, *46*, 764.
(4) Sanchez, E.; Kowalski, B. R. *Anal. Chem.* **1986**, *58*, 496.
(5) Sanchez, E.; Kowalski, B. R. *J. Chemom.* **1988**, *2*, 265.
(6) Burns, D. H.; Callis, J. B.; Christian, G. D. *Anal. Chem.* **1986**, *58*, 1415.
(7) De Ruig, W. G.; Stephany, R. W.; Dijkstra, G. *J. Assoc. Off. Anal. Chem.* **1989**, *72*, 487.

0003-2700/93/0365-1174$04.00/0

$$\mathbf{A} = \begin{bmatrix} \mathbf{a}_1^T & & 0 \\ & \mathbf{a}_2^T & \\ & & \ddots \\ 0 & & \mathbf{a}_p^T \end{bmatrix} \quad (3)$$

when $\mathbf{a}_i$ (i = 1, 2, ..., p) is a short column vector. The right transformation **B** will correct for shift and intensity differences between the columns of $\mathbf{N}_1$ and $\mathbf{N}_2$ (e.g., standardizing the UV order) with the following banded diagonal form

$$\mathbf{B} = \begin{bmatrix} \mathbf{b}_1 & & 0 \\ & \mathbf{b}_2 & \\ & & \ddots \\ 0 & & \mathbf{b}_q \end{bmatrix} \quad (4)$$

where $\mathbf{b}_j$ (j = 1, 2, ..., q) is also a short column vector.

In eq 2, the left transformation **A** is dimensioned as $p \times m$, and the right transformation **B** is dimensioned as $n \times q$, where $p \leq m$ and $q \leq n$. The standardized response $\mathbf{N}_1$ is thus dimensioned as $p \times q$, with the first and last several rows and columns (called missing ends) properly deleted or with extrapolation employed. The selection of p and q is directly related to the bandwidth in **A** and **B** and confined by both the rank of $\mathbf{N}_1$ or $\mathbf{N}_2$ and their original dimensions (m and n). This will be addressed in later sections along with the discussions on a numerical solution for **A** and **B** and their uniqueness.

Once **A** and **B** are calculated from the responses $\mathbf{N}_1$ and $\mathbf{N}_2$ of a common standard sample, any future response $\mathbf{M}_2$ measured on the second instrument can be standardized into the response $\hat{\mathbf{M}}_1$ as if it had been measured on the first instrument using

$$\hat{\mathbf{M}}_1 = \mathbf{A}\mathbf{M}_2\mathbf{B} \quad (5)$$

With $\hat{\mathbf{M}}_1$, this sample can be combined with all other (calibration) samples measured on the first instrument, for the purpose of second-order calibration, library searching, or classification.

Numerical Solution. In the search for a numerical solution for **A** and **B** in eq 2, an iterative alternating least-squares procedure was first used, based on the fact that eq 2 can be reduced to a first-order standardization problem when either **A** or **B** is known. The iteration starts by setting, for example, the left transformation **A** as an identity matrix and uses the first-order PDS[1] to calculate the right transformation **B**, which is then inserted into eq 2 to standardize from the right-hand side. This standardized response can now be used in another first-order PDS to calculate an update for the left transformation **A**. This cycle can be repeated until convergence. Unfortunately, while the iteration does converge, it cannot converge to the correct solution. This is analogous to solving multivariate optimization problems by altering one variable at a time, indicating that the two orders cannot be standardized separately, even in an alternating fashion, and a simultaneous solution for both **A** and **B** is needed.

It is insightful to write out the expression for a typical element in $\mathbf{N}_1$, $\mathbf{N}_{1,ij}$, as a function of a corresponding local submatrix of the elements in $\mathbf{N}_2$ by the use of eq 2

$$N_{1,ij} = \mathbf{a}_i^T \bar{\mathbf{N}}_2 \mathbf{b}_j \quad (6)$$

where

$$\mathbf{a}_i^T = [A_{i\,i-u} A_{i\,i-u+1} \cdots A_{i\,i+v-1} A_{i\,i+v}]$$

$$\mathbf{b}_j = [B_{j-r\,j} B_{j-r+1\,j} \cdots B_{j+s-1\,j} B_{j+s\,j}]^T$$

represent the nonzero elements along the banded main diagonals of **A** and **B**, respectively, and $\bar{\mathbf{N}}_2$ is a $(u + v + 1) \times (r + s + 1)$ submatrix of $\mathbf{N}_2$

$$\bar{\mathbf{N}}_2 = \begin{bmatrix} N_{2,i-u\,j-r} & \cdots & N_{2,i-u\,j+s} \\ \vdots & \cdots & \vdots \\ N_{2,i+v\,j-r} & \cdots & N_{2,i+v\,j+s} \end{bmatrix} \quad (7)$$

Now it becomes clear that, in the second-order standardization given by eq 2, a rectangle in response matrix $\mathbf{N}_2$ is constructed around each corresponding element in $\mathbf{N}_1$ and the left and right transformation vectors, $\mathbf{a}_i$ and $\mathbf{b}_j$, are estimated such that eq 6 is satisfied in a least-squares sense. Recalling that in first-order calibration, a small window is constructed on the second instrument near each specific response channel on the first instrument, it becomes obvious that second-order standardization is a 2D version of PDS. In contrast to first-order PDS, however, all rectangles in 2D PDS are connected with one another through different left and right transformation vectors. For example, $\mathbf{a}_i$ appears in the expressions for *all* elements on the ith row of $\mathbf{N}_1$ and $\mathbf{b}_j$ appears in the expressions for *all* elements on the jth column of $\mathbf{N}_1$. As a result, a numerical solution similar to the moving window method in first-order PDS cannot be devised to produce overall least-squares estimations for these two transformations.

A nonlinear least-squares method is proposed here to solve for all nonzero parameters in **A** and **B** simultaneously. The numerical procedure used is the Gauss–Newton method,[8,9] which requires explicit expressions for first derivatives of all elements in $\mathbf{N}_1$. From eq 6, these first derivatives can be derived as

$$\frac{\partial N_{1,ij}}{\partial A_{i\zeta}} = \sum_{t=i-u}^{i+v} N_{2,\zeta t} B_{tj}$$

where $\zeta \in [i - u, i - u + 1, ..., i + v - 1, i + v]$, and

$$\frac{\partial N_{1,ij}}{\partial B_{\zeta j}} = \sum_{t=i-u}^{i+v} N_{2,t\zeta} A_{it}$$

where $\zeta \in [j - r, j - r + 1, ..., i + s - 1, i + s]$.

For the elements in the first u rows, last v rows, first r columns, and last s columns of $\mathbf{N}_1$, the rectangle in eq 7 cannot be constructed. These elements are therefore ignored in the nonlinear least-squares estimation described above. Alternatively, an extrapolation procedure may be employed. Thus the valid ranges for i and j in eq 6 are $u + 1 \leq i \leq m - v$ and $r + 1 \leq j \leq n - s$, respectively. As a result, p and q in eqs 3 and 4 are given by $p = m - u - v$ and $q = n - r - s$. It should be pointed out that although a constant bandwidth is assumed for both **A** and **B** in the above derivation, **A** and **B** can in fact have varying bandwidths, as long as the uniqueness condition to be discussed in the next section is satisfied.

Uniqueness of Solution. As can be expected, the uniqueness of the nonlinear least-squares solution for **A** and **B** is dependent on the bandwidths in **A** and **B** and the dimensionality of $\mathbf{N}_1$ and $\mathbf{N}_2$. According to the formulation in the previous sections, the total number of unknown parameters (nonzero elements) in **A** and **B** is $p(u + v + 1) + q(r + s + 1)$. Notice in eq 2, the absolute magnitude of the elements in **A** and **B** is undetermined. For example, **A** can be scaled up by a factor while **B** can be scaled down by the

(8) Dennis, J. E., Jr. *Nonlinear Least-Squares State of the Art in Numerical Analysis*; Jacobs, D., Ed.; Academic Press: New York, 1977; pp 269–312.

(9) *Optimization Toolbox (for use with MATLAB™)*; The Math Works Inc.: South Natick, MA, 1991.

same factor without changing the least-squares fit of eq 2. Thus in the calculation, an element of **A** is held constant, for example, by setting $\mathbf{A}_{11} \equiv 1$. Though there are $p \times q$ usable elements in $\mathbf{N}_1$, the number of independent elements in $\mathbf{N}_1$ is limited by its rank and is given as rank $(\mathbf{N}_1) \times \max(m,n)$. Therefore, a necessary and sufficient condition for the uniqueness of a solution is given by the following inequality

$$p(u + v + 1) + q(r + s + 1) - 1 \leq \text{rank}(\mathbf{N}_1) \times \max(m,n) \quad (8)$$

For example, when $m = n = 10$ and $u = v = r = s = 1$ (i.e., **A** and **B** are banded diagonal matrices each with one superdiagonal and one subdiagonal), the uniqueness condition is $\text{rank}(\mathbf{N}_1) \geq 5$. In the case of an LC/UV experiment, this means that a five-component mixture needs to be injected as the standard sample in order to correct for both retention time and specral wavelength shift in a range from −1 to +1 units.

Equation 8 implies that second-order standardization can be accomplished with only one sample, preferably a complicated sample with high rank. Compared to first-order standardization, where multiple standard samples are required, this may be considered as one additional second-order advantage. Of course, when more standard samples are available for standardization, the second-order standardization will be improved. In this case, more equations similar to eq 2 can be included in the nonlinear least-squares estimation, or the sum of all standard samples can be used to replace $\mathbf{N}_1$ and $\mathbf{N}_2$. Since this summed "sample" has a higher signal to noise ratio and possibly a higher rank than $\mathbf{N}_1$ alone, it is expected that eq 2 will become more overdetermined and the nonzero parameters in **A** and **B** can be better estimated.

In case multiple bilinear second-order spectra are available for standardization, there is an alternative approach to calculate the left and right transformations. A trilinear decomposition[10] can be applied to multiple bilinear samples to obtain the resolved pure component spectra **X** and **Y** in both orders. Assuming two bilinear samples (**M** and **N**) are measured on the first instrument as $\mathbf{M}_1$ and $\mathbf{N}_1$, which can be decomposed as

$$\mathbf{M}_1 = \mathbf{X}_1\mathbf{C}_M\mathbf{Y}_1^T$$

$$\mathbf{N}_1 = \mathbf{X}_1\mathbf{C}_N\mathbf{Y}_1^T$$

where $\mathbf{C}_M$ and $\mathbf{C}_N$ are both diagonal matrices with the analyte concentrations in **M** and **N** on the diagonals. When the same two samples are measured on the second instrument, the responses $\mathbf{M}_2$ and $\mathbf{N}_2$ can be similarly decomposed as

$$\mathbf{M}_2 = \mathbf{X}_2\mathbf{C}_M\mathbf{Y}_2^T$$

$$\mathbf{N}_2 = \mathbf{X}_2\mathbf{C}_N\mathbf{Y}_2^T$$

It is seen that the instrumental differences in the **X** order are represented by $\mathbf{X}_1$ and $\mathbf{X}_2$ while the differences in the **Y** order are represented by $\mathbf{Y}_1$ and $\mathbf{Y}_2$. Consequently, the left and right transformations **A** and **B** can be calculated via two separate first-order standardizations as follows

$$\mathbf{X}_1^T = \mathbf{X}_2^T\mathbf{A}^T$$

$$\mathbf{Y}_1^T = \mathbf{Y}_2^T\mathbf{B}$$

For the same example as given above, a sufficient condition for the uniqueness is $\text{rank}(\mathbf{X}_1) = \text{rank}(\mathbf{X}_2) = \text{rank}(\mathbf{Y}_1) = \text{rank}(\mathbf{Y}_2) \geq 3$, which requires less complicated standard samples containing only three components.

(10) Sanchez, E.; Kowalski, B. R. *J. Chemom.* **1990**, *4*, 29.

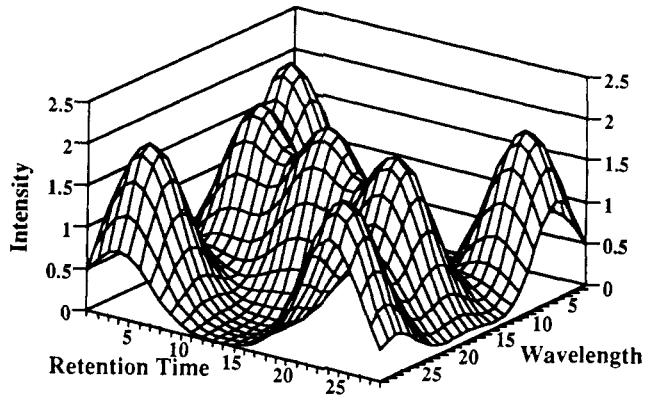

Figure 1. Simulated standard sample response from the first instrument.

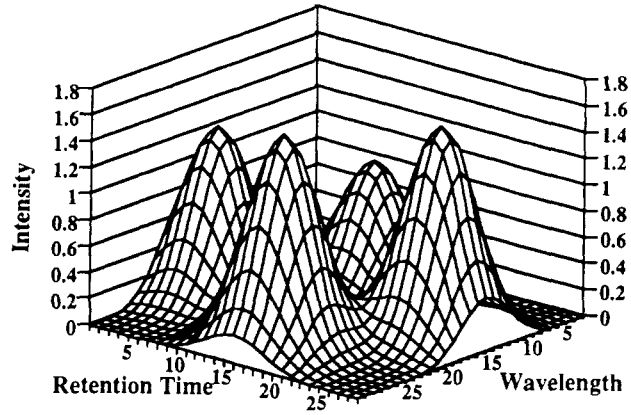

Figure 2. Simulated test sample response from the first instrument.

EXPERIMENTAL SECTION

Computer Simulation of LC/UV Data. The chromatograms and spectra for nine components were generated using Gaussian peaks. Seven out of these nine components were used to generate a bilinear response matrix **N**

$$\mathbf{N} = \sum_{i=1}^{7} c_i\mathbf{x}_i\mathbf{y}_i^T$$

Where $\mathbf{x}_i$'s and $\mathbf{y}_i$'s are the vectors containing pure chromatograms and spectra for these seven components and c_i's are their corresponding concentrations. The remaining two components were combined with two of the components included in **N** to form another bilinear response **M**

$$\mathbf{M} = \sum_{i=6}^{9} c_i\mathbf{x}_i\mathbf{y}_i^T$$

To simulate a deviation from the Lambert–Beer law, the following transformation[11] was carried out for every element in **N** and **M** to generate the true responses $\mathbf{N}_1$ and $\mathbf{M}_1$ on the first instrument (plotted in Figures 1 and 2 respectively),

$$N_{1,ij} = -\log(e^{-N_{ij}} + 0.01) \quad (9)$$

and

$$M_{1,ij} = -\log(e^{-M_{ij}} + 0.01) \quad (10)$$

The responses on the second instrument were simulated through a nonlinear shift of both the chromatographic and spectral axes. This nonlinear shift was generated using a quadratic form $a + bx + cx^2$, where the parameters a, b, and c

(11) Gemperline, P. J.; Long, J. R.; Gregoriou, V. G. *Anal. Chem.* **1991**, *63*, 2313.

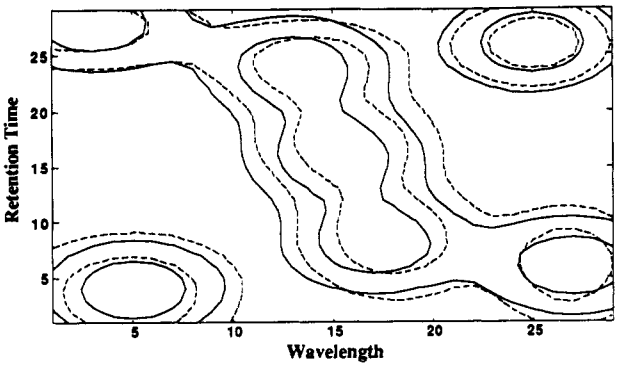

Figure 3. Contour plot of simulated standard sample responses on both instruments (solid line, on the first instrument; dashed line, on the second instrument).

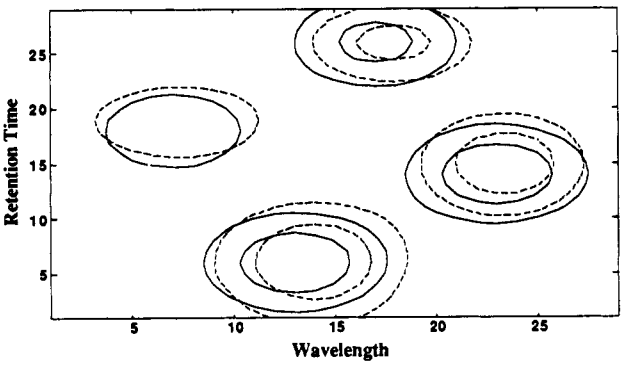

Figure 4. Contour plot of simulated test sample responses on both instruments (solid line, on the first instrument; dashed line, on the second instrument).

were determined such that the shift at both ends was −1 unit while that at the extremes was +1 unit. **N** and **M** were subjected to this shift with linear interpolation to generate the bilinear responses on the second instrument. Following a 10% linear intensity gain, a nonlinear intensity change (approximately 10% of the linear intensity) was simulated by adding 0.03, instead of 0.01, in eqs 9 and 10 to generate the true responses $\mathbf{N}_2$ and $\mathbf{M}_2$ on the second instrument. The responses from the two instruments are overlaid in the contour plots shown in Figures 3 and 4. It is seen that there are significant intensity changes and complicated response channel shifts from one instrument to the other.

In the simulation, $\mathbf{N}_1$ and $\mathbf{N}_2$ were used as the standard sample responses while $\mathbf{M}_1$ and $\mathbf{M}_2$ were used as the test sample responses. Six noise levels, 0.00%, 0.05%, 0.10%, 0.50%, 1.00%, and 5.00%, and eight different types of bands for **A** and **B** were tested in a full factorial design with five repetitions. Since the simulated nonlinear shift was symmetrical in both orders, the same sized band was used for **A** and **B**. In each simulation, **A** and **B** were estimated from the standard sample responses on both instruments and a residual matrix was calculated for eq 2 which indicates the goodness of the model. From this individual matrix, a modeling error was calculated as the mean of the standard deviations of all elements. Similarly, a standardization error could be calculated from the residual matrix for eq 5 with the estimated **A** and **B**. To measure the stability of the proposed parameter estimation method, a standard deviation was also calculated for **A** and **B**, which is the mean standard deviation of all elements in the estimated **A** or **B** (as compared to the **A** and **B** calculated at 0.00% noise level).

LC/UV Experiment. In the LC/UV experiment, a reversed-phase HPLC system was connected to a Hewlett-Packard (Palo Alto, CA) 8452A diode array spectrometer via a flow-through cell. The mobile phase consisted of 60% methanol and 40% 0.005 M tetrabutylammonium sulfate (pH adjusted to 7.0 with $NH_3 \cdot H_2O$). The mobile phase was delivered by two Altex 100A (Altex Scientific, Berkeley, CA) pumps at a total flow rate of 0.4 mL/min and mixed with the injected sample in a mixing chamber before reaching the column and flow-through cell. A Chrompack

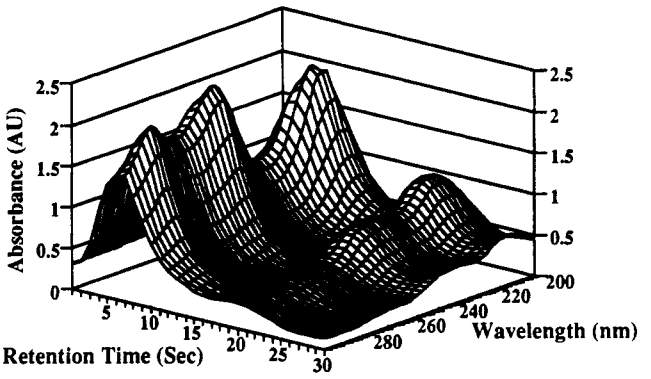

Figure 5. LC/UV response of the standard sample.

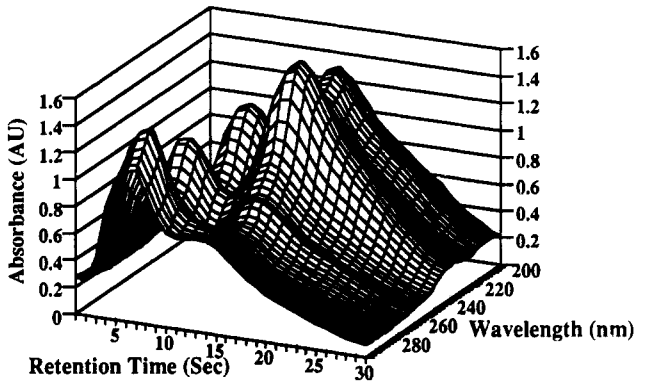

Figure 6. LC/UV response of the test sample.

(Raritan, NJ) reversed-phase C_{18} column was modified to allow the observation of the separation. The injection valve was a pneumatically operated Rheodyne Model 7126 with a 10-μL sample loop. The data collection started 70 s after sample injection at a rate of 1 spectrum/s for a total of 30 s. The spectra were collected in the 200–300-nm range with a 2-nm step.

Four 100 mg/L solutions of FD&C red dye No. 40, blue dye No. 2, yellow dye No. 5, and yellow dye No. 6 were prepared with HPLC-grade water and were then used to prepare two mixtures. The first mixture was prepared by taking 7 mL each of red dye No. 40, blue dye No. 2, and yellow dye No. 5 solutions and diluting to 25 mL with water and serves as the standard sample for standardization. The other mixture was prepared by taking 2 mL of red dye No. 40 solution, 5 mL of blue dye No. 2 solution, and 7 mL of yellow dye No. 6 solution and diluting to 25 mL, which would serve as the test sample for the standardization. In the experiment, a 50-μL sample was injected to fill the sample loop. After the injection of these two samples, the flow-through cell was taken out of the spectrometer. No effort was made to align the flow-through cell in the next run of the same two samples 1 week later. The responses of the two samples measured during the first run are shown in Figures 5 and 6. When these two samples were measured during the second run, the responses became significantly different (shown in Figures 7 and 8). The average difference between the responses of the same sample is ~0.15 AU. Such a dramatic difference would make it impossible to compare and utilize the measurements conducted at a different time.

RESULTS AND DISCUSSION

Computer Simulation. The averaged standard deviations in the estimation of all the nonzero elements in the left and right transformations, **A** and **B**, are plotted in Figures 9 and 10, respectively. From these two figures, it can be seen that more stable estimates of **A** and **B** are obtained with smaller bandwidths, which corresponds to a more overdetermined nonlinear system. This is consistent with the discussion presented in the Theory section, suggesting that a smaller bandwidth is always preferred in terms of parameter estimation. When the band increases to [−2 1] and [−1 2], the

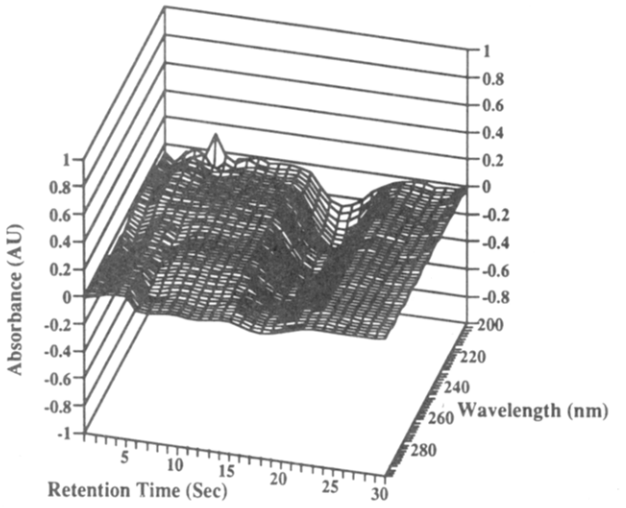

Figure 7. Difference in the responses of the standard sample between two runs.

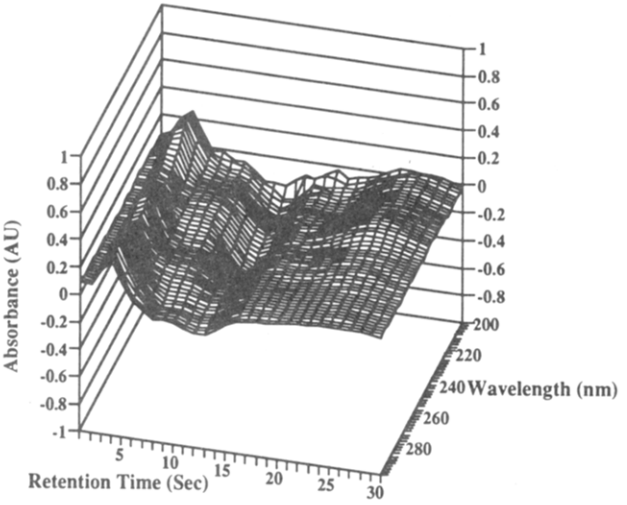

Figure 8. Difference in the responses of the test sample between two runs.

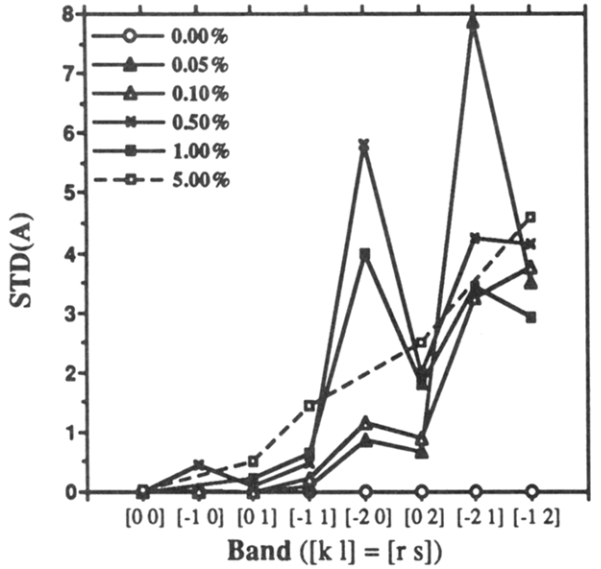

Figure 9. Mean standard deviation in the estimation of left transformation matrix **A** at different noise levels.

mean standard deviation of **A** and **B** undergoes a significant increase, indicating some fundamental change in the system described by eq 2. In fact, referring back to the uniqueness discussion, it is seen that eq 8 is no longer satisfied in these two cases. It is expected that during the parameter estimation

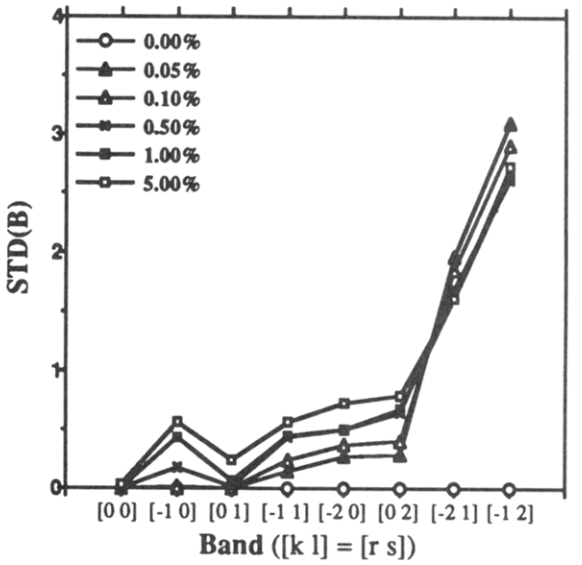

Figure 10. Mean standard deviation in the estimation of right transformation matrix **B** at different noise levels.

the standard deviation will approach infinity, which surprisingly is not the case in Figures 9 and 10. This is believed to be related to the fact that a nonlinearity of the form in eqs 9 and 10 was added, and the effective rank of the response matrix was slightly increased.

When the noise effect is considered, it is seen that the parameter estimation for **A** is relatively stable in the range of 0.00–1.00% noise, while the estimation for **B** seems to be stable in the whole range tested (from 0.00% to 5.00%). When Figure 9 is compared to Figure 10, a much more dramatic fluctuation in **A** is observed. In fact, this fluctuation in **A** is so dramatic at the 5.00% noise level that some of the points had to be left out of the figure. After careful examination, it is found that this dramatic variation comes from the rows in **A** corresponding to the retention times around time 13. Referring back to Figure 1, it is seen that there is only one dominant peak in this region of the response. As a result, the local rank of the response in this region is significantly smaller than the overall rank which determines the uniqueness of parameter estimation, especially when the noise level in the data is high. This explains the poor parameter estimation in **A** at high noise levels. The components are distributed much more evenly along the wavelength axis, and the parameter estimation in **B** becomes more stable. In light of this observation, the standard sample for second-order standardization should be designed in such a way that not only the overall rank satisfies the uniqueness eq 8 but also the local ranks (when examined from both orders) approach this overall rank as much as possible. In other words, the different components in the standard sample should be evenly spread out in the x–y plane.

The modeling error calculated for the standard sample is plotted in Figure 11. In Figure 11, the large error at band [0 0] indicates that a sufficient standardization model has not been obtained. The simulated nonlinear shift is in the [−1 1] range, along with the nonlinear intensity change from instrument to instrument. When one more nonzero diagonal is included in the standardization (at bands [−1 0] and [0 1]), the modeling error is significantly reduced. It is interesting to note that the modeling errors at bands [−1 0] and [0 1] are comparable to each other, showing some form of symmetry. This is consistent with the fact that the shift range is actually [−1 1]. At band [−1 1], the modeling error is further reduced at all noise levels. At the same bandwidth with bands [−2 0] and [0 2], the modeling errors increase only slightly. This suggests that the correction estimation of the range of shifts

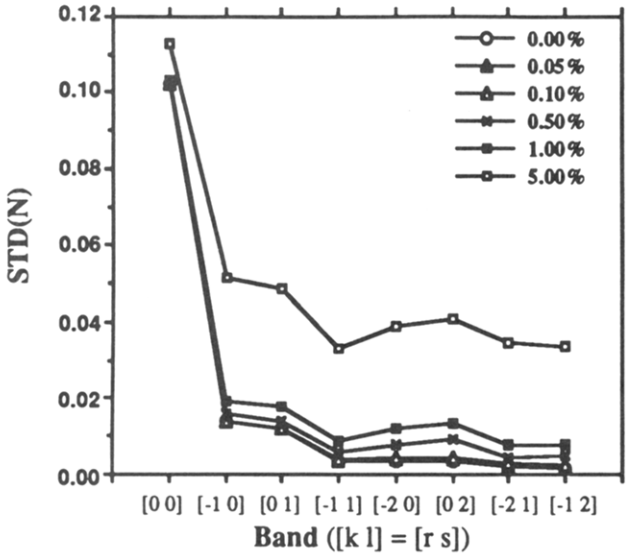

Figure 11. Mean standard deviation in matching the response of the standard sample from the second to the first instrument at different noise levels.

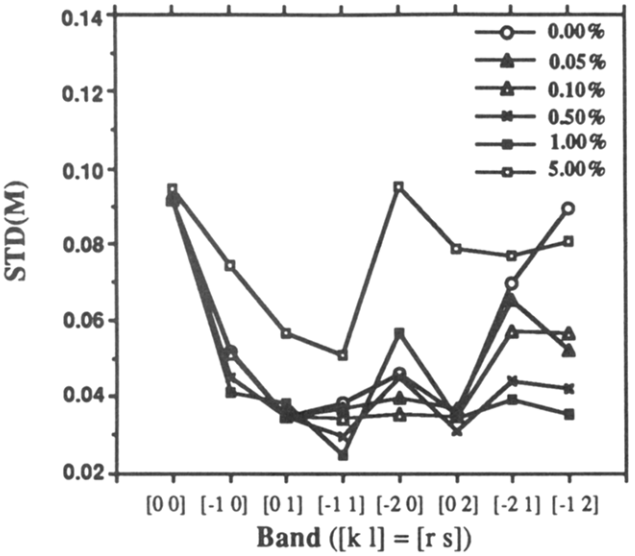

Figure 12. Mean standard deviation in matching the response of the test sample from the second to the first instrument at different noise levels.

in **A** and **B** is not critical owing to the continuity of the responses. When the bandwidth is overestimated by one with the range of shifts included (at bands [−2 1] and [−1 2]), the modeling error is only slightly reduced, indicating that a smaller bandwidth is sufficient to correct for both the nonlinear shifts and nonlinear intensity changes. The symmetry in the modeling error at bands {[−2 0], [0 2]} and {[−1 2], [−2 1]} is also observed. As for the noise sensitivity, it is seen that the modeling error increases slowly as the noise increases from 0.00% to 1.00%. From 1.00% to 5.00% noise, the modeling error is significantly increased, due mostly to the large variance in the estimation of **A**, as has been discussed above. Nonetheless, this can be improved through a better designed standardization sample.

The standardization error calculated from the test sample (Figure 12) shows a pattern similar to that in Figure 11. One difference is that the magnitude of the standardization error is ~2 times that of the modeling error, since the former is prediction error while the latter is just fitting error. Another difference is that the error increases dramatically when the band reaches [−2 1] and [−1 2], especially at higher noise levels, indicating the occurrence of overfitting when an overly

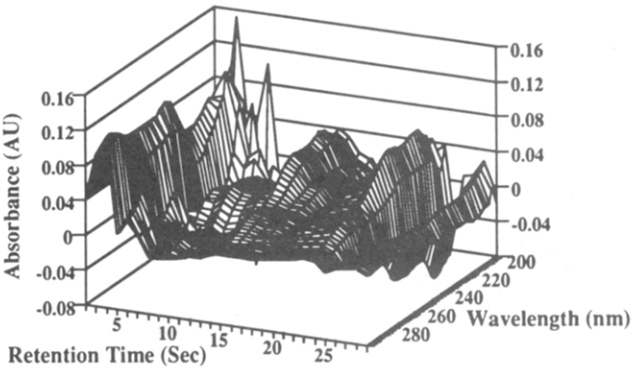

Figure 13. Residual matrix of the standard sample after standardization.

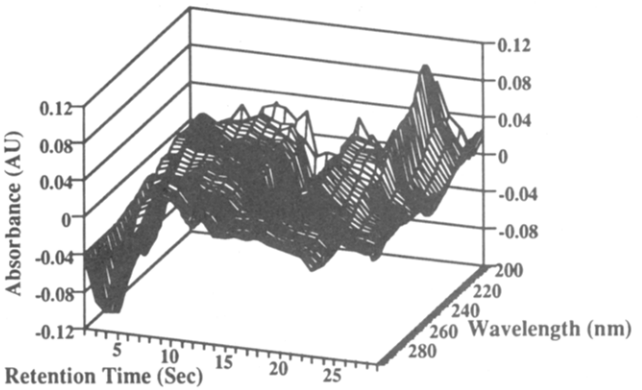

Figure 14. Residual matrix of the test sample after standardization.

large bandwidth is used. In the noise range from 0.00% to 1.00%, the standardization error is relatively stable from band [−1 0] to [0 2]. This is consistent with the discussion above. The standardization error in this range is ~0.04 absorbance unit, which is quite acceptable considering the pronounced difference seen from Figures 3 and 4. The variation pattern of the standardization error at the 5.00% noise level and at bands [−2 1] and [−1 2] is more complicated and less interpretable, due to the enormous variation in the estimation of **A** at the 5.00% noise level (Figure 9) and the large variation in the estimation of both **A** and **B** at bands [−2 1] and [−1 2] (Figure 10). Again, this can be improved by using a better designed standard sample.

LC/UV Experiment. Since the time-dependent response variation in the LC/UV experiment comes mainly from the chromatographic part of the instrument, the band chosen for **B** (spectral order) in the standardization is [0 0] and that chosen for **A** (chromatographic order) is [−1 1]. Figure 13 shows the difference in the sample responses after standardization. It is seen that the difference after standardization is centered around and close to zero in magnitude, indicating that a sufficient model has been attained. However, the residual also shows some clear patterns. There appears to be three bands in the residual, centered around 2, 12, and 20 s in retention time. Referring back to the standard response shown in Figure 5, it becomes clear that the response around 12 s is close to zero and the response around 2 and 20 s corresponds to three similar chromatographic peaks with similar spectral features. As has been discussed in the last section, this will lead to a relatively low local rank and unstable parameter estimations. In spite of this clear pattern, the mean standard error calculated from the difference in the responses has been reduced from ~0.15 (without standardization) to 0.025 after standardization.

For similar reasons, the residual after standardizing the test sample (Figure 14) also shows a pattern around the three retention times mentioned above. The overall trend of the residual is nevertheless centered around and close to zero.

The standard error from standardization is ~0.03. With a better designed standard sample, these clear patterns in the residual can be eliminated and the standardization performance improved.

CONCLUSIONS

The study described in this paper has demonstrated the applicability of the second-order standardization method developed. The computer simulation has indicated the capacity of second-order standardization in modeling both the nonlinear shifts and nonlinear intensity changes, with a relatively small bandwidth for the right and left transformations. In both the computer simulation and the LC/UV experimental data study, the extreme importance of the design of the standard sample is observed. On the other hand, the selection of bands in the transformation matrices can be flexible within a certain range with relatively stable standardization performance. Future research on the second-order standardization should be devoted to error propagation and the optimal design of the standard sample(s).

ACKNOWLEDGMENT

This work was supported by the Center for Process Analytical Chemistry (CPAC), a National Science Foundation Industry/University Cooperative Research Center at the University of Washington. Jim Roe and Caicai Wu are thanked for their help in the LC/UV experimental work.

Received for review October 27, 1992. Accepted January 26, 1993.